Theoretical and Applied Fracture Mechanics 100 (2019) 154–170

Contents lists available at ScienceDirect

Theoretical and Applied Fracture Mechanics

journal homepage: www.elsevier.com/locate/tafmec

Experimental and numerical investigation into the methods of determination of mode I static fracture toughness of rocks

A.M. Pakdaman[a], M. Moosavi[a], S. Mohammadi[b,*]

[a] School of Mining Engineering, Faculty of Engineering, University of Tehran, Tehran, Iran
[b] School of Civil Engineering, Faculty of Engineering, University of Tehran, Tehran, Iran

ARTICLE INFO

Keywords:
Toughness testing of rocks
Fracture process zone
Fracture analysis
Finite element analysis

ABSTRACT

Fracture toughness, as a measure of resistance against crack instability and propagation, is one of the most important parameters in fracture mechanics of rocks and other solid materials. Different methods have so far been proposed in order to determine mode I fracture toughness. In practice, however, considerable differences between their results have been reported. In this study, six conventional tests, including the Single Edge Round Bar Bending test, the Chevron Bend test, the Semi-Circular Bend test, the Straight Notch Disk Bend test, the Brazilian disk test, and the Flattened Brazilian Disk test have been performed on a uniform specimen of gabbro rock for determination of mode I fracture toughness. A notable maximum difference of 42% is observed between the results.

The tests are categorized into three groups in terms of their similarities. Several factors which affect the prediction of fracture toughness are investigated by both the numerical and experimental evidences. Distribution of the fracture process zone around the crack tip, is numerically computed using the 3D finite element analysis and based on both the "normal tensile stress" and the "von-Mises" criteria. According to the investigated features, the Chevron Bend test is the most reliable test for determination of the fracture toughness. Furthermore, the distribution of fracture process zone around the crack tip in this test is non-uniform which leads to over estimation of fracture toughness predicted by the effective crack theory.

1. Introduction

Fracture toughness or critical stress intensity factor represents the material resistance against crack extension and is one of the most important parameters in fracture mechanics of solid materials [1]. For instance, fracture toughness is used to study the rock fragmentation process and classification of rocks [2].

It is generally accepted that an existing crack may behave either in one of the three pure modes of fracture (opening, shearing, and tearing) or in a mixed mode [1,3]. Due to the limitations of rock sample preparation, several methods have been proposed to determine the mode I fracture toughness. In terms of loading, these methods are divided into three categories: tensile, bending and compressive loading conditions [4].

The short rod (SR) test is an ISRM suggested method in which a tensile load is used for determining the mode I fracture toughness [2]. The tests in which the three-point bending are applied to determine the mode I fracture toughness of rocks include the single edge crack round bar bending test (SECRBB) [5,6], the chevron notched short rod bend (CNSRB) method [7], and the ISRM suggested methods of the chevron bend test (CB) [2], and the semi-circular bend test (SCB) [8]. The chevron notch semi-circular bend test (CNSCB) [9], and the straight notch disk bend test (SNDB) [4] are also amongst the proposed methods. The tests that use compressive loading to determine the mode I fracture toughness of rocks are very diverse, but the most important ones are the Brazilian disk test (BDT) [10], the flattened Brazilian disk test (FBD) [11], the cracked straight through Brazilian disc (CSTBD) [12], the modified ring test (MR) [13], and the cracked chevron notched Brazilian disc (CCNBD), suggested by ISRM [14].

Since the fracture toughness is one of the inherent characteristics of materials, fracture toughness values measured from different tests for one type of rock should be in good agreement with each other. Unfortunately, this is not the case in practice. Sun and Ouchterlony based on studies on granite samples concluded that the fracture toughness values of SR samples were more than those of SECRBB samples and once SECRBB samples became pre-cracked, they could provide results closer to SR samples [15]. Also, Khan and Al-Shayea with studies on Saudi Arabia limestone showed that the fracture

* Corresponding author.
E-mail address: smoham@ut.ac.ir (S. Mohammadi).

https://doi.org/10.1016/j.tafmec.2019.01.001
Received 7 October 2018; Received in revised form 22 December 2018; Accepted 6 January 2019
Available online 10 January 2019
0167-8442/

Nomenclature

SR	short rod
ISRM	international society of rock mechanics
SECRBB	single edge crack round bar bending
CB	chevron bend
SCB	semi-circular bend
CNSCB	chevron notch semi-circular bend
SNDB	straight notch disk bend
BDT	Brazilian disk
FBD	flattened Brazilian disk
CSTBD	crack straight through Brazilian disc
MR	modified ring
CCNBD	crack chevron notched Brazilian disc
K_{IC}	mode I fracture toughness
P	load
P_{max}	maximum load
S	distance between supports
D	sample diameter
d	average grain size
Y	dimensionless stress intensity factor of straight notch samples
a	crack length
Y^*	dimensionless stress intensity factor of chevron notch samples
Y^*_{min}	minimum dimensionless stress intensity factor of chevron notch samples
a_0	initial notch length
R	sample radius
B	sample thickness
B_1	crack front
σ_{cr}	$\frac{P_{max}}{2DB}$
K_I	stress intensity factor
c	half of crack length
α	half of loading angle
$B^{'}$	in case of Brazilian disk is equal to $920\,m^{-3/2}$
Φ	dimensionless stress intensity factor of BDT and FBD samples
Φ_{max}	maximum dimensionless stress intensity factor of BDT and FBD samples
P_{min}	local minimum point in the recorded load-displacement curve
MTS	material testing systems
SENB	single edge notched beam
W	sample width
a_1	maximum depth of chevron flanks
FPZ	fracture process zone
f_t	tensile stress of rock
S Mises	Von-Mises stress
S normal	the stress normal to the crack plane

toughness values obtained from the CSTBD samples were less than those of the CCNBD samples [16]. They also stated that among the fracture toughness values in straight notch samples obtained from SCB, SECRBB and CSTBD tests, the SCB and CSTBD tests reported the highest and lowest values for fracture toughness, respectively [16].

The study of Chang et al. on granite and marble samples showed that there was a good agreement in fracture toughness values of CCNBD, CNSCB and BDT tests, all were clearly more than the SCB value. The reason was believed to be due to non-pre cracking of SCB samples [17]. Iqbal and Mohanty, who were studying on three types of granite, noted that using $\frac{1}{\sqrt{R}}$ instead of $\frac{1}{\sqrt{D}}$ in the ISRM suggested equation in the CCNBD test, determined a better fracture toughness value [18,19]. Later, however, Wang et al. discussed that the experimental equation of Iqbal and Mohanty [18,19] could not be confirmed theoretically [20,21]. Study on sandstone samples by Cui et al. showed that the fracture toughness value of CCNBD samples was 8–27% less than the fracture toughness in SR samples with the same diameter of CCNBD samples [22]. They used the suggested equation of Iqbal and Mohanty [18,19] to calculate the fracture toughness and noted that, better agreement would be achieved for larger diameters [22]. The numerical investigation of Dai et al., which simulated progressive fracturing during the CCNBD test, manifested that the straight-through assumption would not be achieved during the test, affecting the accuracy of fracture toughness [23]. Recently, Wei et al. clarified the controversial issue about the conservative fracture toughness of the CCNBD method [24 and 25]. They used the distribution of acoustic emission to show the existence of a large FPZ [24]. Furthermore, by recalculation of the dimensionless stress intensity factor in three standard chevron-notched tests (i.e. the CB, SR, and CCNBD) and numerical estimation of the length of FPZs, they demonstrated that underestimation of the minimum dimensionless stress intensity factor in the ISRM-suggested method and the large fracture process zone were the two major reasons of lower fracture toughness values in the CCNBD test [25]. In another research, Tutluoglu and Keles demonstrated that the fracture toughness values of SCB samples of andesite and marble were less than those of the CCNBD samples [4]. They also stated that the fracture toughness of SNDB samples with ratio of thickness to radius equal to 1, was approximately equal to fracture toughness of SCB samples [4]. Moreover, fracture toughness of SNDB samples with ratio of thickness to radius more than 2, was similar to that of CCNBD samples [4]. They also applied the equation of Iqbal and Mohanty [18,19] to calculate the fracture toughness [4]. Recently, Funatsu et al. also noted that in the sandstone samples the fracture toughness of the SCB test was less than the value of the CB test [26]. They stated that using the K-resistance curve for determining fracture toughness of the SCB samples would lead to results close to the second level values of fracture toughness in CB samples [26]. While Wei et al. showed that the straight-through assumption in the chevron notch might cause some errors due to the curved crack front in CNSCB samples [27], Wei et al. used the same assumption to present a wide range of fracture toughness values in this test [28].

In this paper, six tests i.e. CB, SECRBB, BDT, FBD, SCB, SNDB are performed on a uniform gabbro rock to investigate the range of differences obtained in mode I test results by these methods. Then, the tests are modeled numerically after sufficient verifications. The tests are categorized into similar groups and the experimental and numerical results are investigated to determine the influencing factors and their effects. Finally, general comparisons are conducted to better determine the reliability of each test. The process is typically shown in Fig. 1.

2. Fracture toughness determination tests

2.1. Single Edge crack round bar bending test (SECRBB)

Ouchterlony used this method to determine the fracture toughness of Marble. The main feature of this method is to use core samples of rocks in which a straight notch is cut (Fig. 2). The equation proposed to determine the fracture toughness is [6]:

$$K_{IC} = 0.25\left(\frac{S}{D}\right)Y\frac{P_{max}}{D^{1.5}} \quad (1)$$

where P_{max} is the maximum load, (S/D) is the ratio of span to diameter, Y is the dimensionless stress intensity factor, D is the sample diameter and K_{IC} is the mode I fracture toughness. The Y factor clearly varies

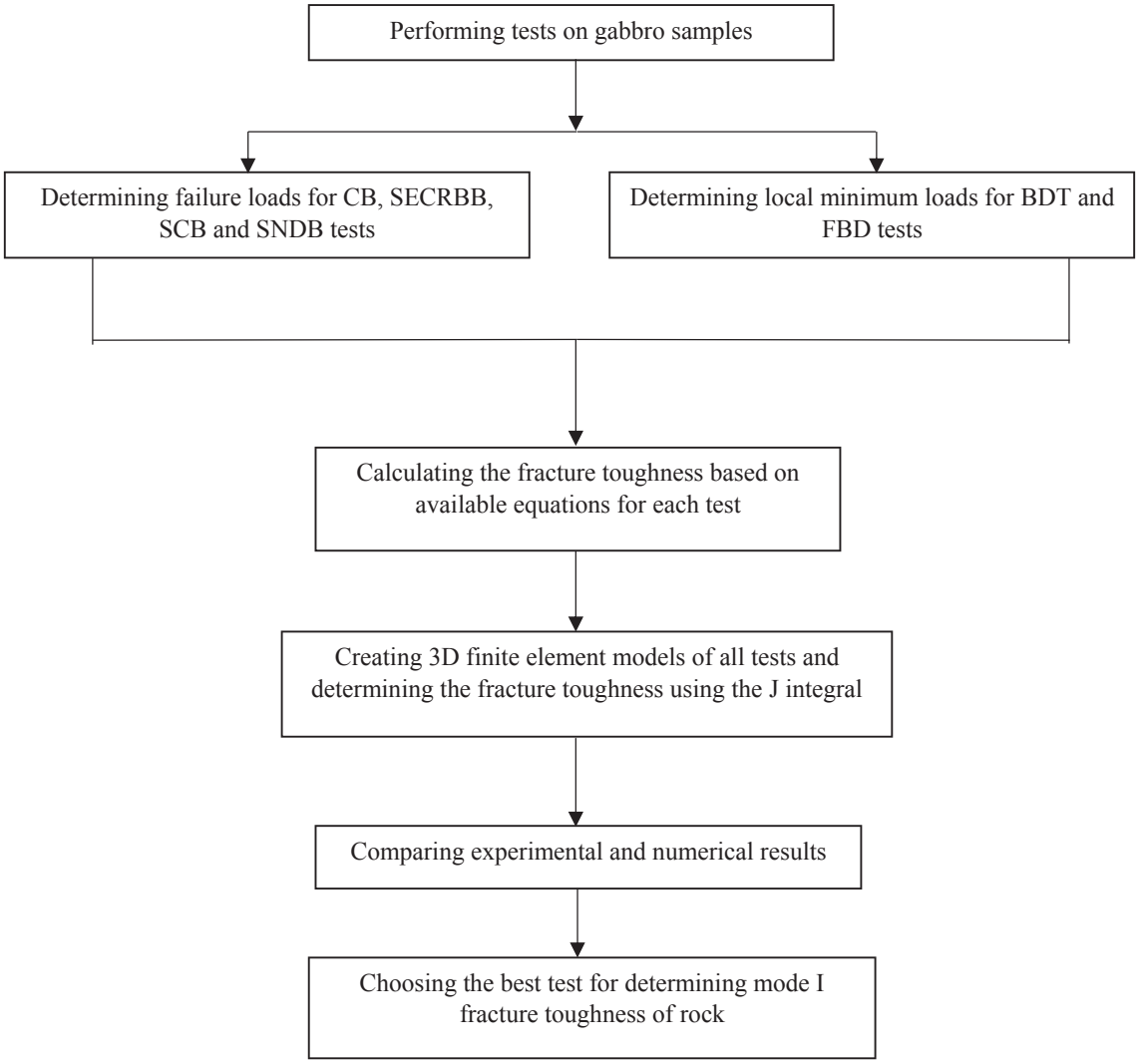

Fig. 1. Procedure for choosing the best test for determining the fracture toughness.

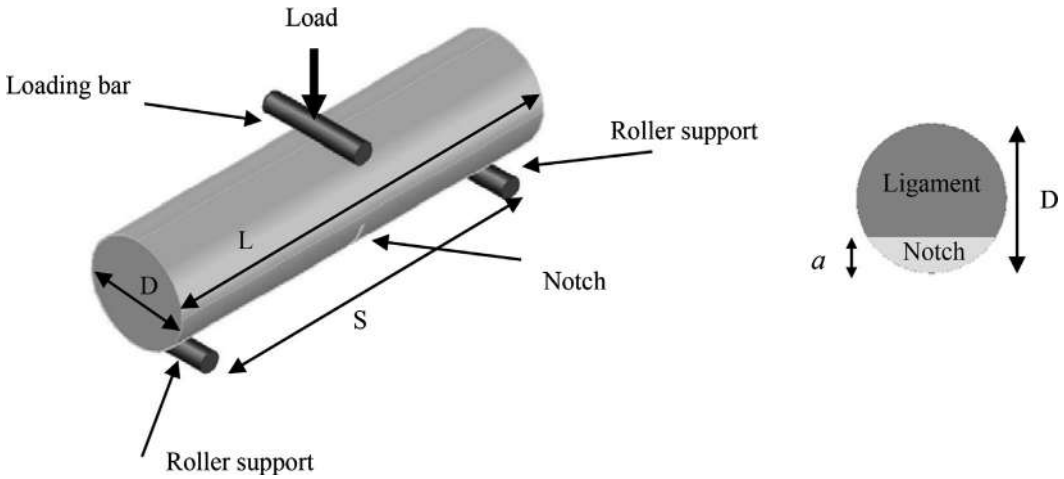

Fig. 2. Single Edge Crack Round Bar Bending (SECRBB) test specimen.

with the ratio of (S/D). For $(S/D) = 3.33$, this parameter is defined as Eq. (2):

$$Y = \frac{12.7527\left(\frac{a}{D}\right)^{0.5}\left[1 + 19.646\left(\frac{a}{D}\right)^{4.5}\right]^{0.5}}{\left[1 - \frac{a}{D}\right]^{0.25}} \tag{2}$$

where a is the length of notch.

2.2. Chevron bend test (CB)

This test is one of the ISRM suggested methods for determining the fracture toughness [2]. In this test, a notch is created in the center of core and in the beam span. The created notch is in the form of a V shape, called the chevron notch (Fig. 3). Dimensions of the notch are obtained from the ISRM-suggested method [2].

This test is carried out in two levels. In the first level, only the failure load is recorded while in the second level, the full load-displacement curve is recorded with the help of a stiff loading frame. The second level of the test is used only if the sample shows a significant non-linear behavior. Therefore, the first level of the test is sufficient for the present study. The rock fracture toughness is determined by the following equation [2].

$$K_{IC} = \frac{Y^*_{min} P_{max}}{D^{1.5}} \tag{3}$$

where P_{max} is the maximum load, D is the diameter of the sample, and $Y^*_{min}$is the minimum dimensionless stress intensity factor, defined by [2]:

$$Y^*_{min} = \left[1.835 + 7.15\frac{a_0}{D} + 9.85\left(\frac{a_0}{D}\right)^2\right]\frac{S}{D} \tag{4}$$

where S is the distance between supports and a_0 is the length of initial notch.

2.3. Semi circular bend test (SCB)

This test was designated in 2014 as an ISRM method for determining the mode I fracture toughness. In this test, the core is divided into 2 halves (Fig. 4). Eq. (5) is used to determine mode I fracture toughness [8].

$$K_{IC} = Y\frac{P_{max}\sqrt{\pi a}}{2RB} \tag{5}$$

where P_{max} is the maximum load, a is the notch length, R is the radius of semicircle, B is the sample thickness and Y is the dimensionless stress intensity factor [8]:

$$Y = -1.297 + 9.516\left(\frac{S}{2R}\right) - \left(0.47 + 16.457\left(\frac{S}{2R}\right)\right)\beta + \left(1.071 + 34.401\left(\frac{S}{2R}\right)\right)\beta^2 \tag{6}$$

Here, β is the ratio of notch length to the disk radius, and S is the support span.

2.4. Straight notch disk bend test (SNDB)

This is one of the newest tests proposed by Totluoglu and Keles to determine the fracture toughness of rock samples [4]. The test includes a cylindrical disk sample whose center is notched along the sample length, as depicted in Fig. 5. Eq. (7) is used to determine the fracture toughness of sample [4].

$$K_{IC} = Y\sigma_{cr}\sqrt{\pi a} \tag{7}$$

where $\sigma_{cr} = \frac{P_{max}}{2DB}$ is the critical stress, a is the notch length, D is the diameter of the sample, P_{max} is the maximum load, B is the sample thickness and Y is the dimensionless stress intensity factor which should be calculated numerically by Eq. (8),

$$Y = \frac{K_I}{\sigma_{cr}\sqrt{\pi a}} \tag{8}$$

and K_I is numerically evaluated from the J-integral.

2.5. Brazilian disk test (BDT)

In 1993, Guo et al. presented the Brazilian test for determining the fracture toughness of rock samples. No initial notch is required in this test (Fig. 6) [10].

The test terminates after the maximum load where a local minimum drop is observed in the loading. There is no need to record the full load-displacement curve in this test. The fracture toughness of the samples is determined from Eq. (9) [10]:

$$K_I = B^{'}P\Phi\left(\frac{c}{R}\right) \tag{9}$$

where c is the half of final crack length, P is the applied load, R is the radius of disc and α is the half of the loading angle. $\Phi\left(\frac{c}{R}\right)$ is the dimensionless stress intensity factor and is equal to 0.112 for $\alpha = \pm 5°$. The value of B' is equal to 920 $m^{-3/2}$. In case of different dimensions, values of Φ and B' can be determined from [10]. K_I is the stress intensity factor which represents the fracture toughness if the local minimum point is reached. For the case of above stated dimensions, Eq. (9) can be simplified to Eq. (10):

$$K_{IC} = 104.1P_{min} \tag{10}$$

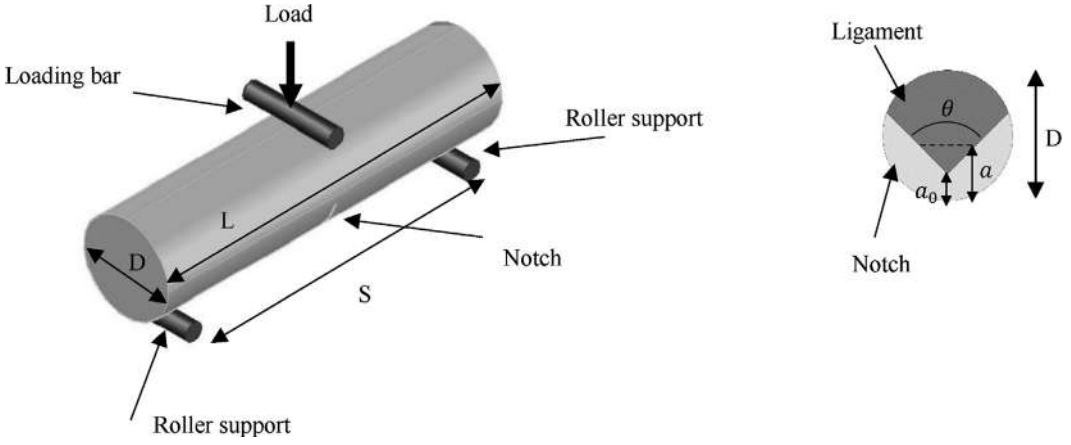

Fig. 3. Chevron bend (CB) test specimen.

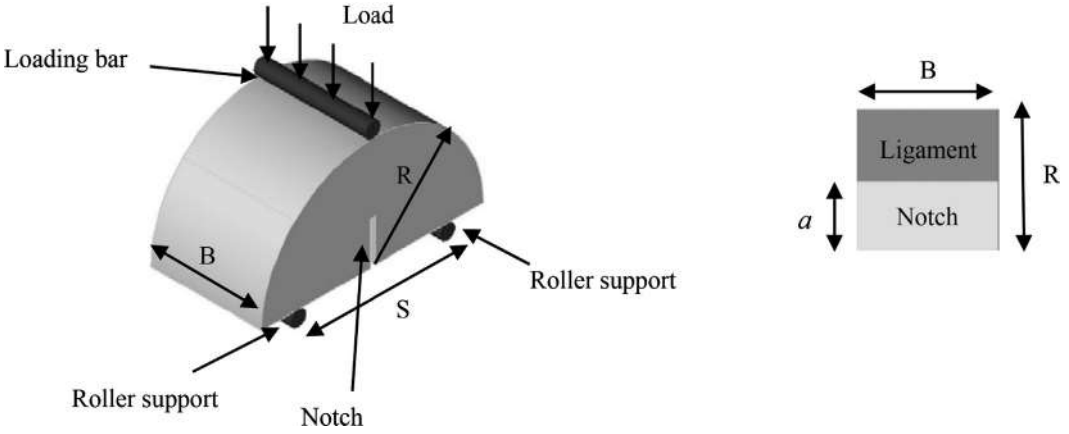

Fig. 4. Semi Circular Bend (SCB) test specimen.

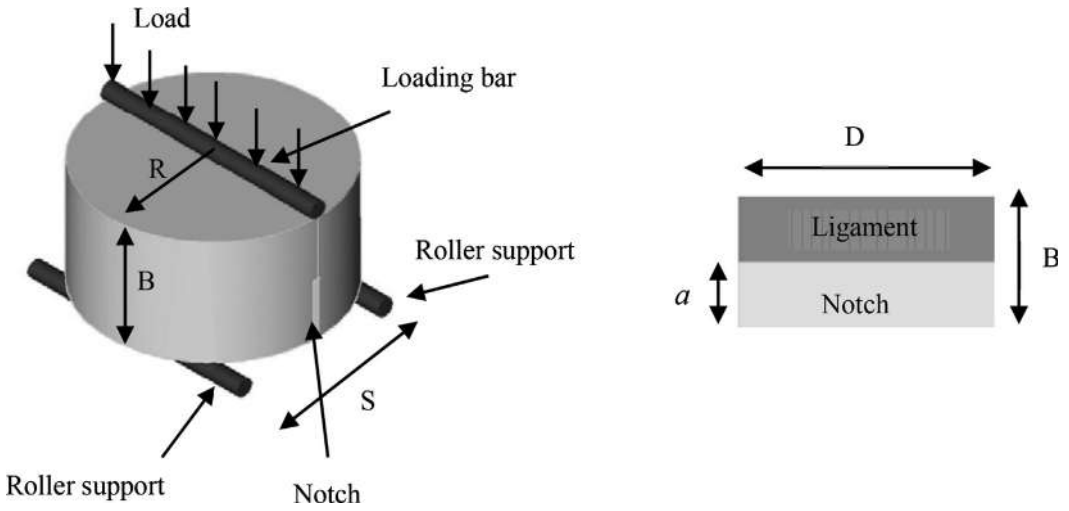

Fig. 5. Straight Notch Disk Bend (SNDB) test specimen.

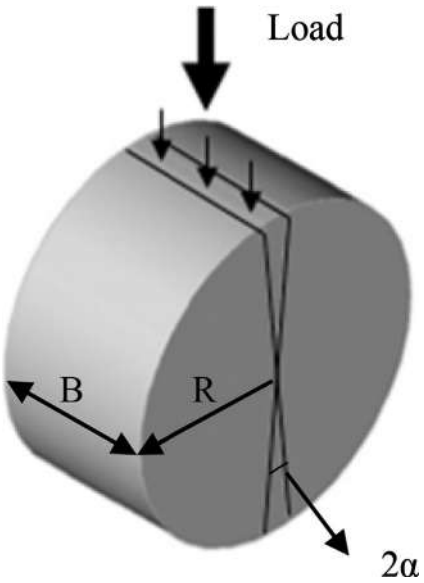

Fig. 6. Brazilian Disk (BDT) test specimen.

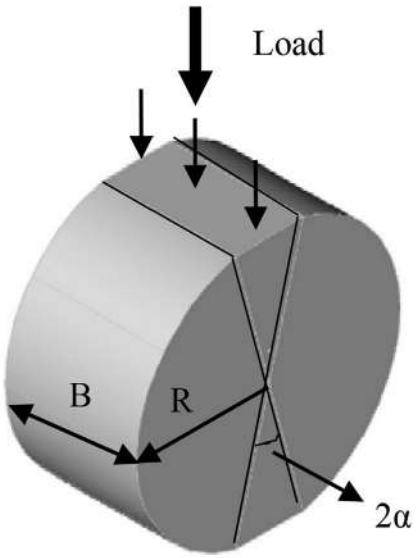

Fig. 7. Flattened Brazilian (FBD) test specimen.

where P_{min} is the local minimum point in the recorded load-displacement curve.

2.6. Flattened Brazilian test (FBD)

This test was proposed by Wang and Xing to improve the Brazilian test for determining the fracture toughness. In this method, the Brazilian test sample is flattened at both ends to simplify the application of loading (Fig. 7). The crack initiation occurs at the center of the disk, which depends on the angle of loading [11].

In this test, it is only required to record the local minimum point of the load-displacement curve. Eq. (11) is used to evaluate the fracture toughness:

$$K_{IC} = \frac{P_{min}}{\sqrt{R}B}\Phi_{max} \tag{11}$$

where R is the radius of disc, Φ is the dimensionless stress intensity factor with the maximum value of Φ_{max}, B is the sample thickness and P_{min} is the local minimum point of the load-displacement curve. Φ_{max} is determined numerically for each angle of loading. Wang et al. used the finite element and boundary element methods to obtain $\Phi_{max} = 0.58$ for flattened Brazilian disk samples for the loading angle $2\alpha = 30°$ [11,29]. Also, Keles and Tutluoglu calculated the maximum dimensionless stress intensity factor as 0.445 for $2\alpha = 30°$ by using the two-dimensional finite element analysis [30].

3. Experiments

Gabbro samples were chosen for performing fracture toughness tests in the Rock Mechanics Laboratory of University of Tehran. Mineralogical and mechanical properties of the gabbro samples are mentioned in Tables 1 and 2, respectively.

Higher values of notch thickness can increase fracture toughness values [31]. However, Justo et al. performed 216 fracture toughness tests on four rock types with different notch radii from 0.15 mm to 15 mm under 4-point bending conditions, and demonstrated that for notch radii less than a critical distance, usually a few mm in rocks, variation of the notch thickness does not change the fracture toughness significantly [31]. The critical distance in rocks is usually surrounded by the grain size and ten times of this parameter [32]. In addition, the ISRM suggested method states the saw thickness for straight notch tests should be less than the average size of the grains [8]. Accordingly, the saw thickness in this study was chosen 1.58 mm.

Servo-controlled material testing machine, MTS 815, was used to load the samples. All experiments were performed at a speed of 0.002 mm/s in order to avoid the effects of loading rate and dynamic effects on fracture toughness. A load cell with capacity of 5 ton was used to record the test loading. In each test type, three tests were performed to determine the fracture toughness accurately.

Samples with 54 mm diameter, 216 mm length and 180 mm support distance (S/D = 3.33) and straight notch with 11.7 mm length were used to determine the fracture toughness in SECRBB test. Samples with 54 mm diameter, 216 mm length and 180 mm support distance (S/D = 3.33) were used in the CB test. The chevron notch angle was 90° and the initial length of notch was 11 mm. In SCB test, semicircle samples were used with 74 mm diameter, 37.5 mm thickness and 50 mm span length and straight notch with 15 mm length. In the SNDB test, cylindrical samples were used with 74 mm diameter, 37.5 mm thickness and 50 mm span length and straight notch with 18 mm length. For the BDT test, samples with 54 mm diameter, 27 mm thickness and the contact angle of jaws with samples about 10° ($\alpha = 5°$), were tested to determine fracture toughness. Finally, same samples were used in the FBD test with 54 mm diameter and 27 mm thickness, flattened at both ends with an angle of 30° ($2\alpha = 30°$).

Table 3 summarizes the result of performed tests. The fracture toughness in all tests is determined using the already available reference equations, except in the SNDB test in which no analytical equation is available and a numerical modeling is adopted. Fig. 8 shows the fractured samples of different tests.

4. Numerical modelings

Three-dimensional finite element method based on singular elements for crack tip modeling is used to simulate the tests. The fracture toughness is determined from the J integral. Only half of the sample in SECRBB, CB, SCB, SNDB tests and a quarter of sample in BDT and FBD tests are modeled due to symmetry to reduce the size of the model. Experimentally obtained failure loads for CB, SECRBB, SCB, SNDB tests and local minimum loads in BDT and FBD tests are used for determining the fracture toughness in models. Also, fracture toughness and stress intensity factors are determined with 10 contours around the crack tip. In straight notch tests (i.e. SECRBB, SCB, and SNDB), the fracture toughness is calculated around the notch crack tip. However, for remaining tests (i.e. CB, BDT, and FBD), the toughness is computed for the critical stress induced crack length in which the dimensionless stress intensity factor reaches its critical value. Reliability of this numerical approach has been confirmed by several researches [4,7,25,28,30,33]. Mesh arrangement includes 15-node quadratic triangular prisms around the crack tip and 20-node quadratic bricks elsewhere. In order to verify the numerical modeling procedure, the one Single Edge Notched Beam test (SENB) sample is modeled and the numerical results are compared with the analytical solutions. After verifying the procedure, the main tests are modeled and discussed.

4.1. Verification based on the Single Edge notched beam test (SENB)

A cubic block of 45 cm length, 10 cm width and 10 cm thickness is used to model the SENB sample (Fig. 9). The length of cracks varies from 20 to 80 mm. Approximately, 7800 elements and 35,000 nodes are used in the model. A dimensionless stress intensity factor, independent of the applied load, is adopted. This method is only used for verification of numerical models, and it is not included in the experimental tests of Section 3. The numerically evaluated dimensionless stress intensity factor (Eq. (12)), determined from 10 contour integrals around the crack tip for a constant load, is compared with the analytical solution (13) presented by [1]. The applied load is 1000 N (500 N for half of the model because of symmetry).

$$Y = \frac{K_I BW^{1.5}}{PS} \tag{12}$$

$$Y = \frac{3\sqrt{\frac{a}{W}}\left[1.99 - \left(\frac{a}{w}\right)\left(1 - \frac{a}{W}\right)\left(2.15 - 3.93\left(\frac{a}{W}\right) + 2.7\left(\frac{a}{W}\right)^2\right)\right]}{2\left(1 + 2\left(\frac{a}{W}\right)\right)\left(1 - \frac{a}{W}\right)^{3/2}} \tag{13}$$

where a is the crack length, W is the sample width, K_I is the stress intensity factor, B is the sample thickness, P is the applied load and S is the supports span.

Fig. 10 demonstrates the adopted finite element mesh for simulation

Table 1
Mineralogical information of gabbro samples.

Plagioclase (%)	Amphibole (%)	Biotite (%)	Mafic minerals (%)	Apatite (%)	The average grain size (mm)
80–85	10–15	2–3	3–5	< 1	2

Table 2
Properties of gabbro samples.

Young's modulus (Gpa)	Poisson's ratio	Density (gr/cm^3)	Uniaxial compressive strength (MPa)	Tensile strength (MPa)	Porosity (%)
42.98	0.18	2.85	132.15	11.12	0.24

of the SENB test which is finer around the crack tip and coarser elsewhere. Variation of the dimensionless stress intensity factor as a function of the ratio of crack length to sample width for the block samples is shown in Fig. 11. It indicates that the difference between numerical and analytical results is less than 2%, which proves the accuracy of numerical modeling.

Fig. 11. Shows that the variation of dimensionless stress intensity factor is ascending, a sign of unstable crack growth in the specimen. During crack propagation, and according to Eq. (14) and Fig. 11, an ascending trend is observed for variation of the dimensionless stress intensity factor in terms of the crack length. As a result, lower load is required for a specific critical stress intensity factor in longer crack length during crack propagation; an indication of decreasing trend for the required failure load during crack propagation, or an unstable crack growth. A similar argument was provided by [28].

$$K_{Ic} = \frac{P_{max} S}{BW^{1.5}} Y \tag{14}$$

4.2. Numerical modeling of single edge crack round bar bending test (SECRBB)

5600 elements and 25,000 nodes are used to model the SECRBB test. Six different levels of increasing crack length are considered to represent the crack growth. The dimensionless stress intensity factor is calculated for each constant load and the obtained values are compared with the results of Eq. (2). In these samples, due to the ascending curve of the dimensionless stress intensity factor, the crack growth is unstable. Fig. 12 shows a very good agreement between the numerical modeling and analytical solution up to the ratio of crack length to sample diameter equal to 0.65. The reason for this might be due to the fact that the proposed equation by Ouchterlony is valid only for the range of crack length to sample diameter ratios of 0 to 0.6. The fracture toughness determined by the numerical modeling is 2.285 $MPa\sqrt{m}$, with a difference of less than 1 percent (0.185%) with Eq. (1).

4.3. Numerical modeling of the Chevron bend test (CB)

The model for CB specimen for 6 different lengths of crack front (the crack front is shown in Fig. 13) include approximately 7200 elements and 31,200 nodes. The results of Fig. 14 show that there is a minimum point on the curve of variations of the dimensionless stress intensity factor in terms of the dimensionless crack length, which is an indication of the critical crack length. Before this point, the crack extends in a stable regime, and afterward the crack extension becomes unstable. The crack front propagation is illustrated in Fig. 15. The fracture toughness based on the minimum point is 2.5 MPa$\sqrt{m}$, which shows 8% difference with Eq. (3). A similar discrepancy between FEM models and the ISRM suggested equation for determining the fracture toughness was also reported in [25].

4.4. Numerical modeling of the semi circular bend test (SCB)

6 different levels of increasing crack length are modeled by 14,500 elements and 62,300 nodes. The dimensionless stress intensity factor is calculated for one constant load and it is compared with the reference ISRM values of Eq. (6). Due to the ascending form of Y factor, as shown in Fig. 16, samples show unstable crack growth. According to Fig. 16, the agreement of the results is good for the ratio of crack length to the sample radius in the range of 0.4–0.6, but they have remarkable differences for ratios greater than 0.6. This is expected as ISRM suggests that Eq. (6) is only valid in the range of 0.4–0.6. The fracture toughness calculated from the numerical modeling is 1.62$MPa\sqrt{m}$, which has 2.4% difference with the ISRM value (Eq. (5)). The reason may be attributed to the fact that the ISRM equation was derived for plane strain condition, which is different from the present 3D model.

4.5. Numerical modeling of the disk sample test with straight notch (SNDB)

For modeling the crack growth, four different levels of increasing crack length are used on a model of 9300 elements and 40,100 nodes. The dimensionless stress intensity factor is calculated for one constant load. The ascending shape of the Y curve indicates the unstable crack growth (Fig. 17). Unfortunately, no analytical solution is available to compare and verify the numerical results. The fracture toughness is measured to be 1.97$MPa\sqrt{m}$.

4.6. Numerical modeling of the Brazilian test (BDT)

A quarter of the disk is modeled with similar dimensions of the experimental samples. A finite element mesh of 6200 elements and 27,300 nodes are generated for the modeling and 9 different levels of increasing crack length are considered. The modeling begins from the point of fracture initiation, which is considered at the center of the disk. Fig. 18 shows the variation of dimensionless stress intensity factor with the ratio of crack length to radius. Accordingly, the curve shows two trends: before the maximum point (unstable crack growth) and after it (stable crack growth). This maximum point is used for determination of the fracture toughness.

According to Fig. 18, the numerical and analytical results are in a good agreement for small crack lengths (less than 10 mm or c/R = 0.37). However, for larger crack lengths, a considerable difference exists with the maximum values of 0.112 and 0.248 for the dimensionless stress intensity factor in the analytical solution and numerical modeling, respectively. The analytical results for half crack lengths (which are longer than 10 mm (or c/R = 0.37)) are not reliable due to the assumption of infinite plate, as noted earlier by Wang and Xing [11]. Therefore, wherever the crack is too long (the half crack length is longer than 10 mm or c/R = 0.37), the analytical solution (Eq. (9)) can no longer be used. The maximum value of the dimensionless stress intensity factor occurs at c/R = 0.85, which is very close to the

Table 3
Values of mode I fracture toughness obtained from the tests.

Test name	Failure load (kN)	Fracture toughness (MPa.$\sqrt{m}$)	Test name	Local minimum load (kN)	Fracture toughness (MPa.$\sqrt{m}$)	
SECRBB	5.42	2.29	BDT	20.64	2.11	
CB	2.77	2.72	FBD	21.61	Wang et al. [11,29]	2.71
SCB	4.69	1.58			Keles and Tutluoglu [30]	2.08
SNDB	8.92	1.97				

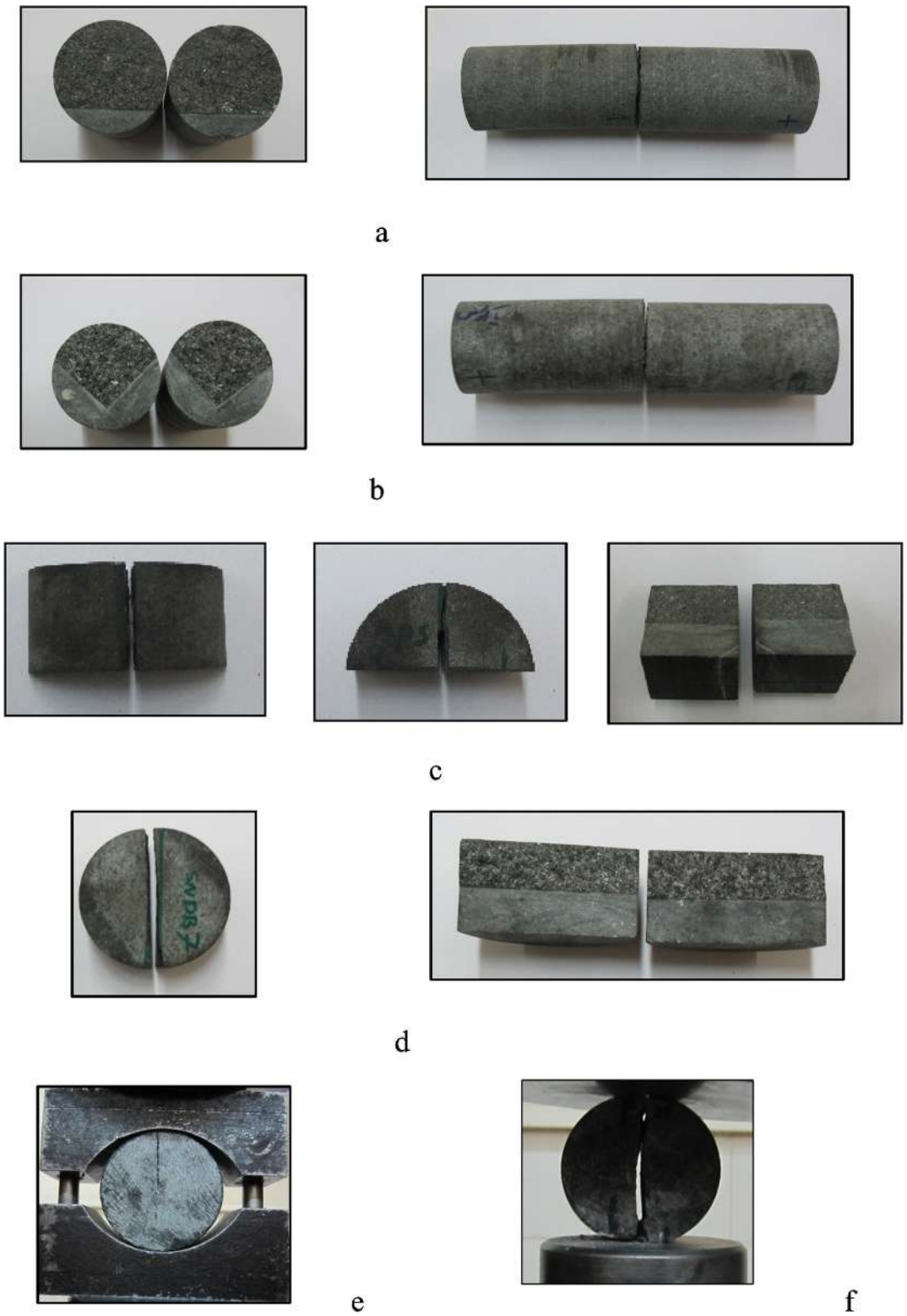

Fig. 8. Fractured samples. (a) SECRBB test (b) CB test (c) SCB test (d) SNDB test (e) BDT test and (f) FBD test.

loading surfaces. The calculated fracture toughness is $4.75MPa\sqrt{m}$.

4.7. Numerical modeling of the flattened Brazilian test (FBD)

In both Brazilian and flattened Brazilian test models, an initial crack exists in the model and the way it is extended is examined. Wang et al. [11,29], and Keles and Tutluoglu [30] used the Griffith criterion to indicate that in disks with 30° flattened angle, crack extension would occur from the center of the sample. For modeling the crack growth, 9 different levels of increasing crack length are used on a model of approximately 7400 elements and 32,300 nodes. According to Fig. 19 and similar to the Brazilian test, variation of the dimensionless stress intensity factor shows two trends: before the maximum point (unstable crack growth) and after the maximum point (stable crack growth). The

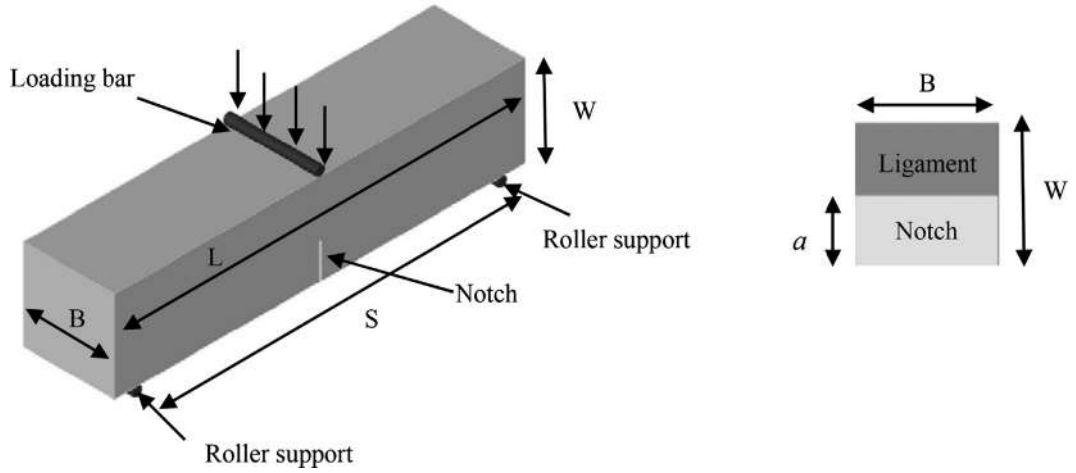

Fig. 9. Single Edge Notched Beam Test (SENB) test specimen.

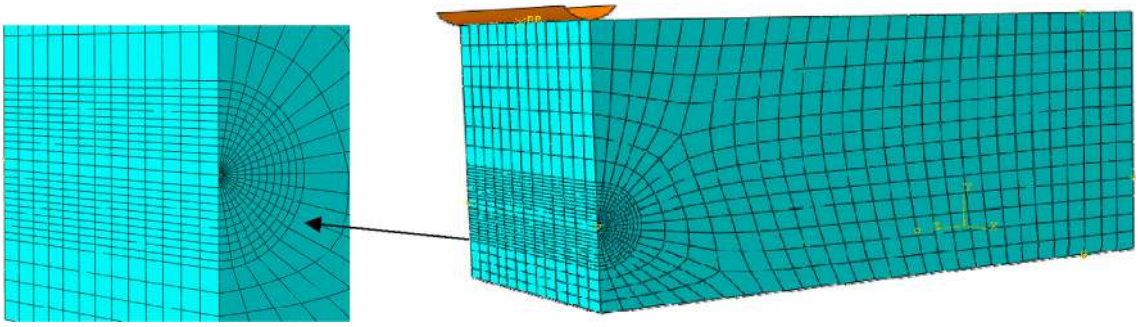

Fig. 10. Finite element mesh of the SENB test.

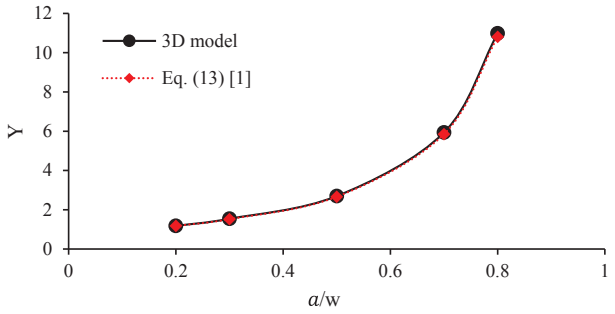

Fig. 11. Comparing the analytical and numerical values of the dimensionless stress intensity factor in the SENB test.

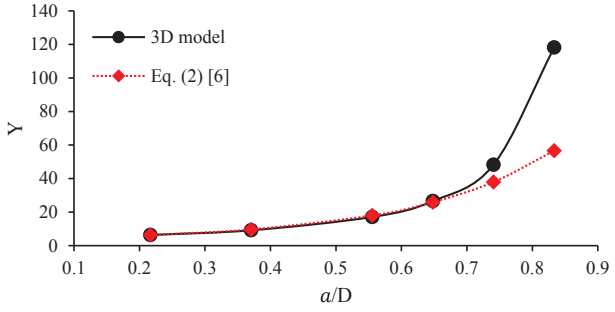

Fig. 12. Comparing the analytical and numerical values of dimensionless stress intensity factor in the SECRBB test.

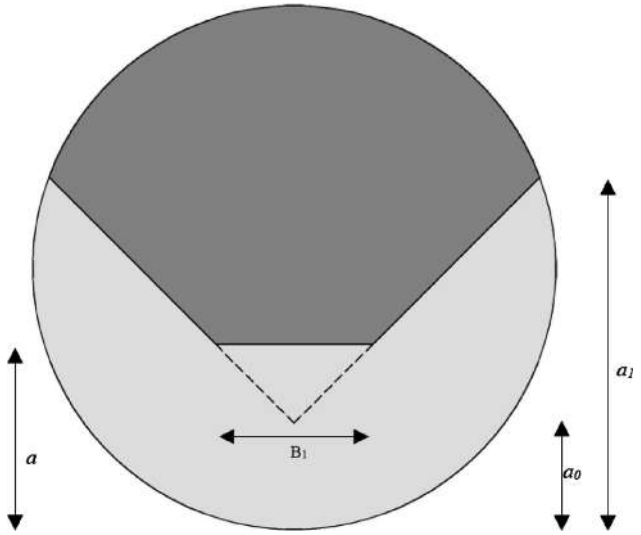

Fig. 13. Schematic view of the crack front B_1 and the crack length a.

fracture toughness is calculated at the maximum point of the curve, which is associated with 18 mm crack length (c/R = 0.67). Therefore, the corresponding position is close to the loading surfaces.

The maximum dimensionless stress intensity factor is 0.47, which is close to 0.445, achieved by Keles and Tutluoglu [30]. The insignificant differences are due to the differences in the three-dimensional solution in this paper and two-dimensional plane strain solution of Keles and Tutluoglu [30]. The maximum value occurs in the ratio of crack length to radius (c/R) equal to 0.67. The fracture toughness is measured to be $2.2MPa\sqrt{m}$, with the difference of 5.3% with the value reported by

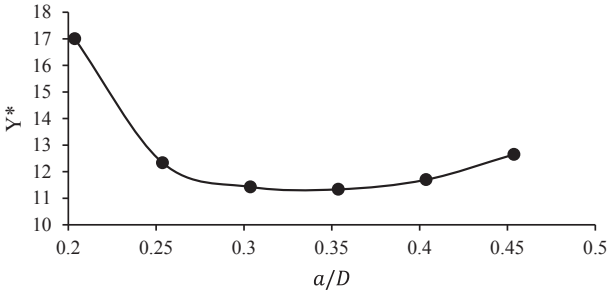

Fig. 14. Variation of the dimensionless stress intensity factor of the CB specimen for different crack fronts.

Keles and Tutluoglu [30]. Again, there is no analytical solution for comparison.

5. Discussion on experimental and numerical results

Comprehensive results and discussions in sections 3 and 4 clearly indicate that the values of fracture toughness depend on various factors such as shape and dimensions of sample, type of notch, sample thickness, stability of crack extension, size of fracture process zone, loading conditions, and so on. In order to better examine these effects, samples are divided into 3 similar groups:

1. CB and SECRBB samples: The difference between these two samples is just the type of notch.
2. SCB and SNDB samples: Only differ in their shapes.
3. BDT and FBD samples: Flattening is the only source of difference.

5.1. Comparison of CB and SECRBB samples

Despite the fact that the test failure load in samples with chevron notch is lower than samples with straight notch, the values of fracture toughness of CB samples are greater than values obtained by SECRBB samples. Stable crack growth in CB samples is one of the most important advantages of this type of notch compared with SECRBB samples.

In order to determine the fracture process zone in all tests, first, the corresponding equivalent stress is evaluated based on the linear elastic assumption. Then, the points with levels above the yield stress are considered as part of fracture process zone.

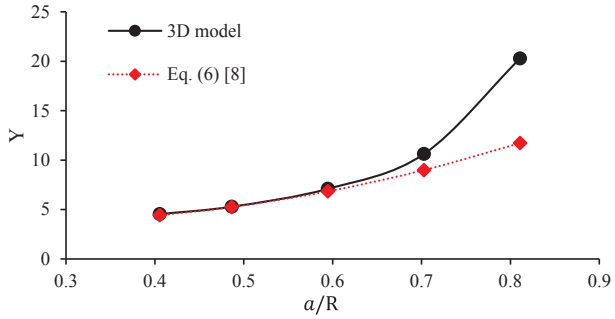

Fig. 16. Comparing the values of dimensionless stress intensity factor in the SCB test.

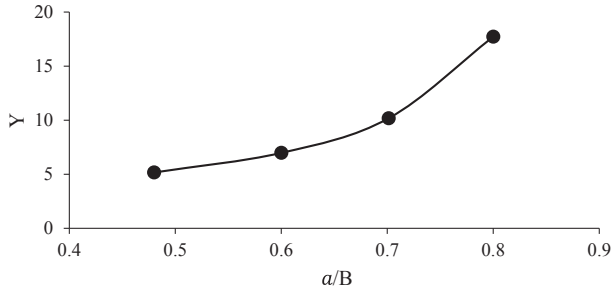

Fig. 17. Dimensionless stress intensity factor of the SNDB specimen for different values of a/B.

Two criteria are used to estimate the fracture process zone: the uniaxial normal tensile stress criterion, and the von-Mises multiaxial criterion. According to the brittle behavior of rocks and assuming that the tensile yield stress of rock is equal to the tensile strength, each part of the sample with stresses greater than the tensile strength is assumed to be part of the fracture process zone, which develops due to subcritical stable crack growth. The stress normal to the crack plane and the equivalent von-Mises stress of the two criteria are compared with the tensile strength of rock. The size of the fracture process zone is determined along two axes at the center and corner of the samples. In the SECRBB test, the center of the notch and 15.57 mm out of the center are chosen. In the CB test, similarly, two axes at the center of the crack

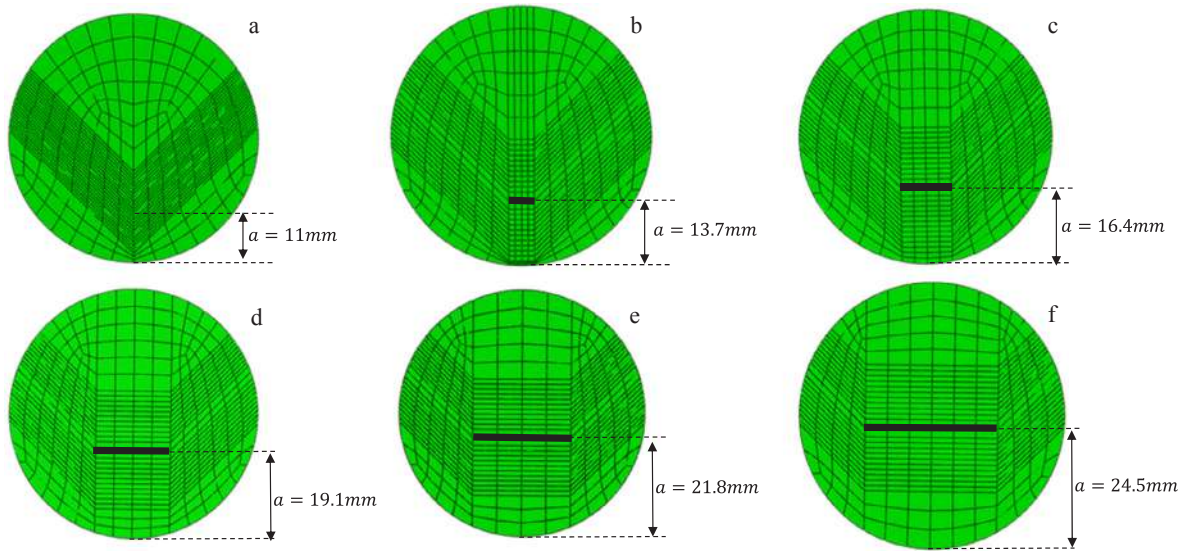

Fig. 15. Position of the crack front during crack propagation in the cross section of the chevron notch samples (the bold line shows the crack front length) a: $B_1 = 0$ b: $B_1 = 5.4$ mm c: $B_1 = 10.8$ mm d: $B_1 = 16.2$ mm e: $B_1 = 21.6$ mm f: $B_1 = 27$ mm.

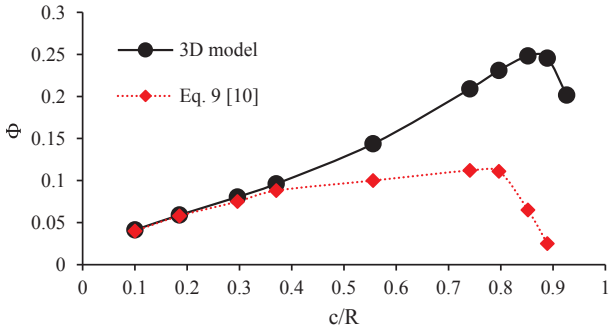

Fig. 18. Comparing the analytical and numerical values of dimensionless stress intensity factor in the BDT test.

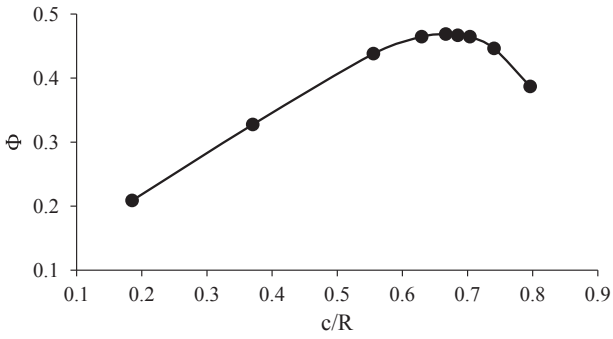

Fig. 19. Variation of the dimensionless stress intensity factor for the FBD specimen for different values of c/R.

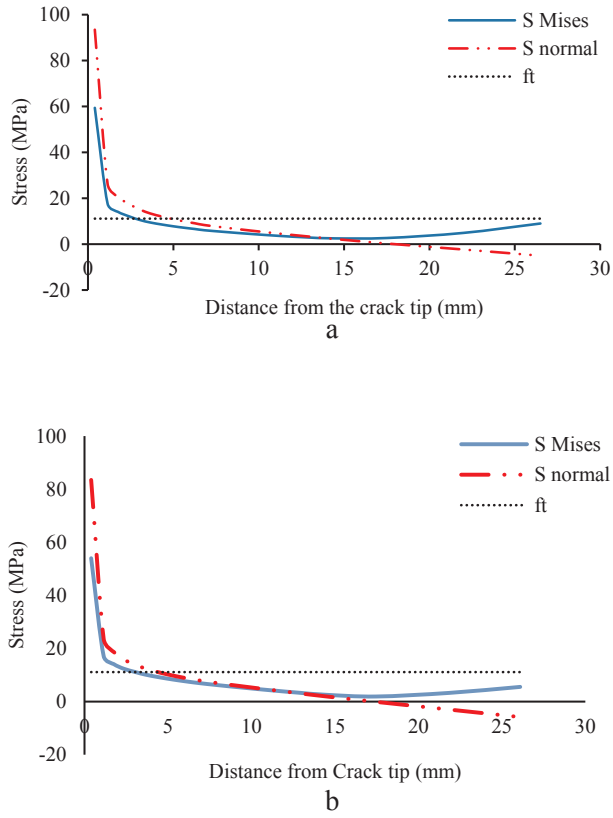

Fig. 20. Profile of stress variation from the crack tip in the SECRBB test, (a) Center of the sample and (b) Corner of the sample.

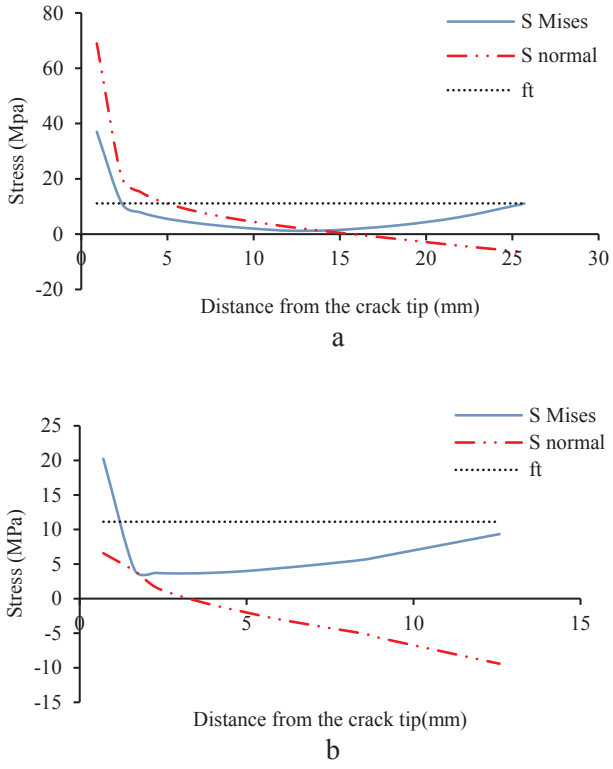

Fig. 21. Profile of stress variation from the crack tip in the CB test, (a) Center of sample and (b) Corners of sample.

front inside the notch, and 26.38 mm away from the center along the crack front (which corresponds to the minimum dimensionless stress intensity factor) are considered.

According to Figs. 20 and 21, the normal tensile stress criterion predicts a similar 5 mm fracture process zone length in the center of both notch types, but in the corners of SECRBB sample, the length of the fracture process zone is 4.6 mm, while it is zero in CB samples. Based on the von-Mises criterion, the length of the fracture process zone is 2.5 mm at center of samples for both notches, but in the corners of SECRBB samples, the FPZ length remains unchanged. In CB samples the length of FPZ is reduced to 1.25 mm and is eventually eliminated. The length of the fracture process zone at the center of the CB sample (5 mm) is in a good agreement with the equation proposed in [25] for estimation of the fracture process zone based on the normal tensile stress criterion in the CB test (5 mm). Fig. 22 shows the fracture process zone around the crack tip in SECRBB and CB samples.

It is also noted that a limited localized compressive stress zone can be observed around the loading points and supports, as depicted in Fig. 22c,d. It is, however, not considered as a fracture process zone.

The shape of fracture process zone is assumed to be circular (in reality it is dumbbell shape). According to the normal tensile stress criterion, the ratios of volume of fracture process zone to the total volume of SECRBB and CB samples are 0.71 and 0.38 percent, respectively. The same ratios become 0.18 and 0.13 percent based on the von-Mises criterion. Therefore, the size of fracture process zone in SECRBB samples are greater than CB samples. Fig. 22c,d shows the extent of fracture process zone in SECRBB and CB samples on the crack plane based on the von-Mises criterion, which clearly predicts a dumbbell-shape for both samples. Figs. 20, 21, and 22 show that while the distribution of the fracture process zone around the crack tip is approximately uniform in SECRBB samples, it does not remain uniform in the chevron notch samples.

The CB test produces more accurate value for the fracture toughness than the SECRBB test because of its stable crack growth, which results

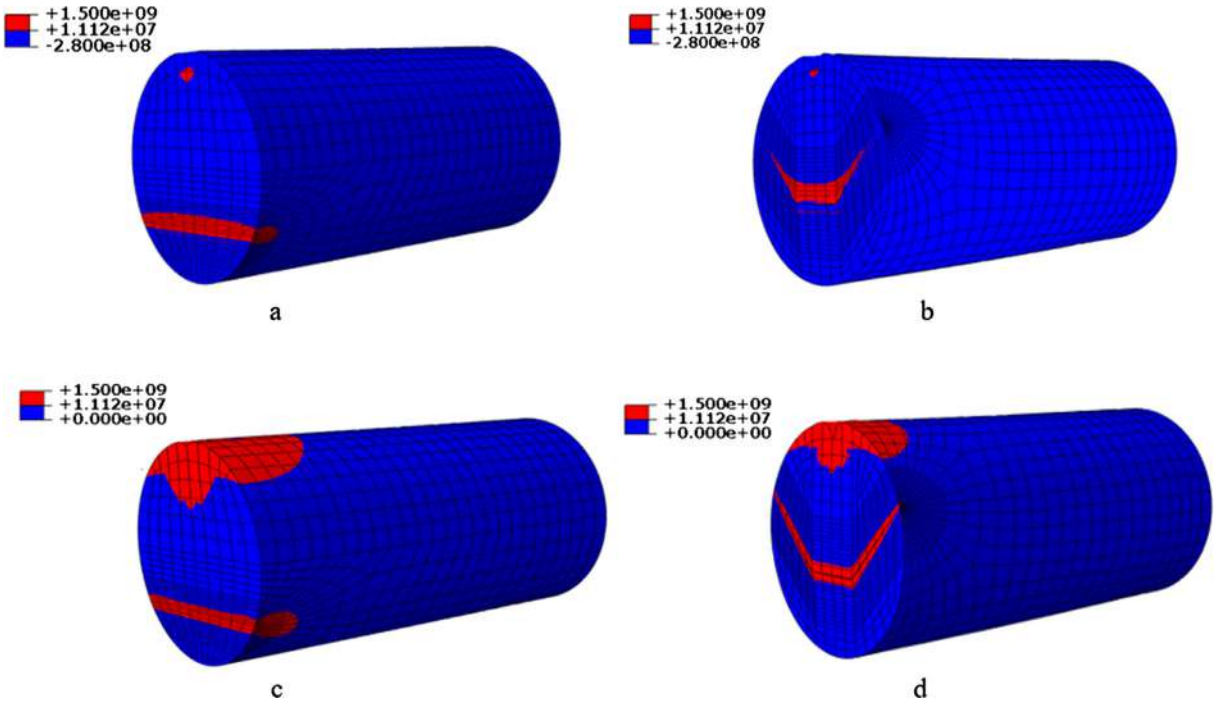

Fig. 22. Numerically predicted fracture process zones in the cylindrical samples, (a) SECRBB samples based on the normal tensile stress criterion (b) CB samples based on the normal tensile stress criterion, (c) SECRBB samples based on the von-Mises criterion and (d) CB samples based on the von-Mises criterion (The red zone around the crack tip is the FPZ). (For interpretation of the references to colour in this figure legend, the reader is referred to the web version of this article.)

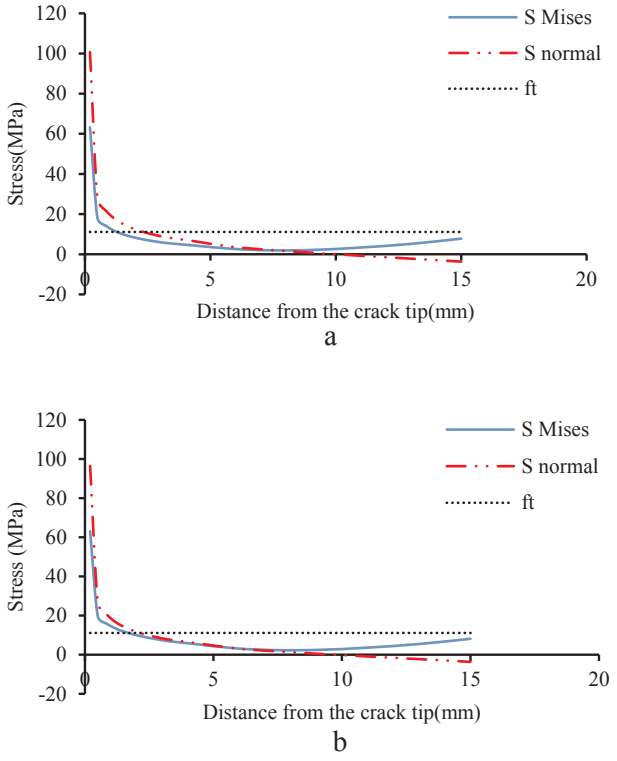

Fig. 23. Profile of stress to distance from the crack tip in the SCB test, (a) Center of sample and (b) Corners of sample.

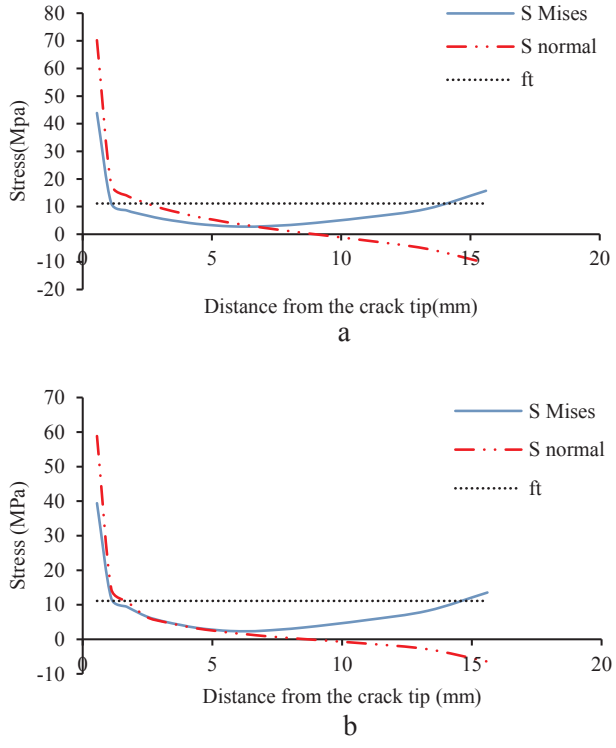

Fig. 24. Profile of stress to distance from the crack tip curve in the SNDB test, (a) Center of sample and (b) Corners of sample.

in creation of a sharp and narrow crack on the top of notch and smaller size of the fracture process zone, better matching of the linear elastic assumption. Although the straight-through assumption may have some limits in determining the fracture toughness in chevron notched samples [23,27], this assumption has been broadly used to determine fracture toughness values [7,25,28,33].

5.2. Comparison of SCB and SNDB samples

Geometric characteristics of both SNDB and SCB samples are similar. In both samples, the thickness and radius are the same and there

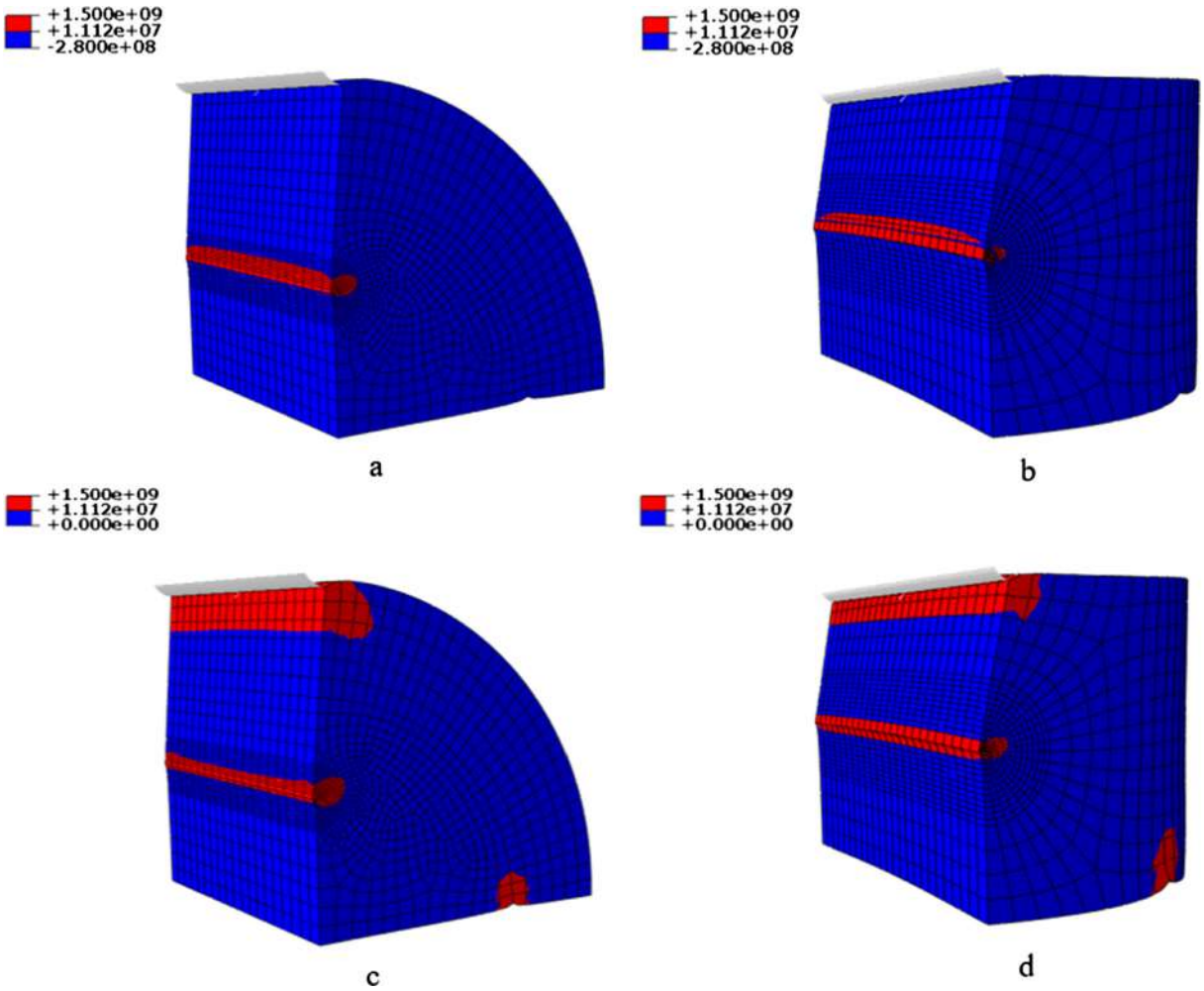

Fig. 25. Numerically predicted fracture process zones in SCB and SNDB samples, (a) SCB samples based on the normal tensile stress criterion (b) SNDB samples based on the normal tensile stress criterion, (c) SCB samples based on the von-Mises criterion and (d) SNDB samples based on the von-Mises criterion (The red zone around the crack tip is the FPZ). (For interpretation of the references to colour in this figure legend, the reader is referred to the web version of this article.)

may only be an insignificant difference between the notch lengths. Failure load in SNDB samples is approximately twice of SCB samples and the fracture toughness of SNDB samples is almost 20% greater than SCB samples. In both tests, the dimensionless stress intensity factor follows an ascending trend, so unstable crack growth occurs in both cases. Two axes are specified to determine the size of the fracture process zone. The first axis is at the center of the notch in both samples while the second axis is 32.38 mm and 15.58 mm out of the center in SNDB and SCB samples, respectively.

The length of fracture process zone based on the normal tensile stress criterion at the center and corners of SCB sample is 2.5 mm, while it is 2.5 mm and 1.7 mm, respectively, at the center and corners of the SNDB experimental samples. It should be stated that the length of the fracture process zone predicted by the normal stress criterion in the SCB test is very close to the prediction of [33] (2.68 mm). According to the von-Mises criterion, the FPZ length at the center and corners of SCB samples is 1.25 mm and 1.8 mm, respectively, but it is 1.5 mm at the center and corners of SNDB samples. With the assumption of circular FPZ (although it is a dumbbell-shape), the ratio of the volume of fracture process zone to the total volume of the sample based on the normal tensile stress criterion for SCB and SNDB samples is 0.91 and 0.64 percent, respectively, while the von-Mises criterion predicts it 0.34 and 0.19 percent, respectively. In both criteria, the fracture process zone is greater in the SCB samples. Figs. 23 and 24 illustrate variation of stress with respect to distance from the crack tip. In addition, the distribution of the fracture process zone in the SCB and SNDB samples was illustrated in the Fig. 25.

Similar to the previous tests, some compressive stress is observed near the loading point (Fig. 25c,d), which cannot be considered as a fracture process zone.

According to the normal tensile stress and von-Mises criteria, the fracture process zone around the crack tip in SCB samples is greater than in SNDB samples. Since the linear elastic assumption is more accurate for SNDB samples, the fracture toughness obtained from this test is more accurate than the typical semicircular samples. As shown in Fig. 25c,d, induced fracture process zone in SCB and SNDB samples around crack tip based on the von-Mises criterion is dumbbell-shape.

5.3. Comparison of BDT and FBD samples

As mentioned in Section 4.6, the assumption of infinite plate in deriving a relation for evaluation of the stress intensity factor is inconsistent with the limited dimensions of the Brazilian disk. On the other hand, in the BDT test, the crack initiates from the loading surfaces (as discussed by [11,29,30]) which does not produce a pure tensile mode. Also, Wang and Xing [11] noticed that the BDT test lacks the uniform distribution of the load on the disk. Therefore, it can be concluded that the fracture toughness values obtained from the BDT test are less reliable. Therefore, FBD samples are used to determine the fracture toughness in which fracture initiates from the center of sample

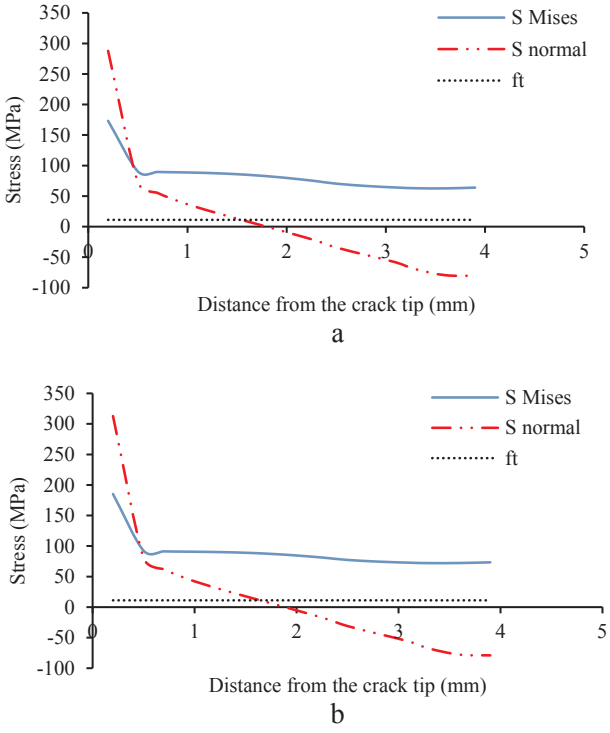

Fig. 26. Profile of variation of stress to distance from the crack tip in the BDT test, (a) Center of sample and (b) Corners of sample.

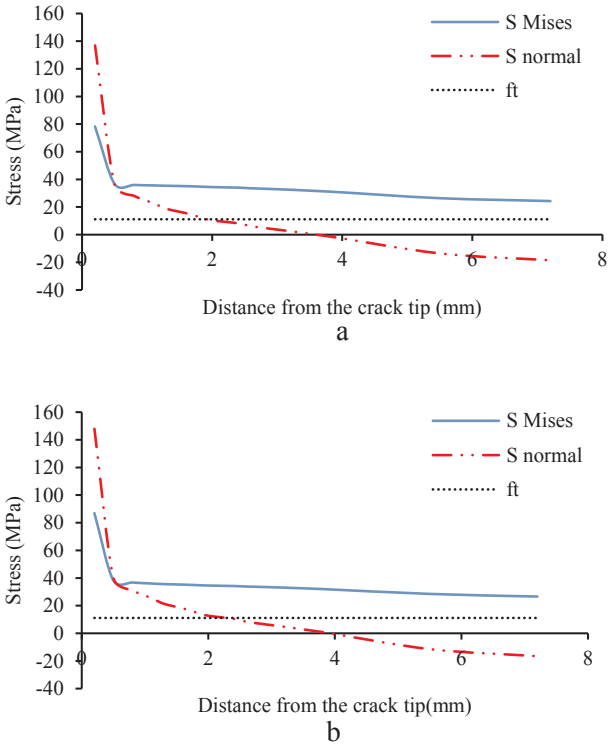

Fig. 27. Profile of variation of stress to distance from the crack tip in the FBD test, (a) Center of sample and (b) Corners of sample.

under a special loading angle and the distribution of load remains uniform on the end surfaces. On the other hand, the equation for evaluation of the stress intensity factor is based on the assumption of a finite plate [29,30]. In both tests, the normal tensile stress and von-Mises criteria are used to estimate the size of the fracture process zone. Estimation of the fracture process zone in this test is carried out at the c/R value, which corresponds to the maximum dimensionless stress intensity factor. Two axes at the center and corner of the critical crack are chosen for determining the length of the fracture process zone. The corner axes in BDT and FBD tests are at 10.61 mm and 10.80 mm out of the center of the critical crack.

Figs. 26 and 27 illustrate that the lengths of fracture process zone around the crack tip (according to the normal tensile stress criterion) at the center and corners of BDT and FBD samples are 1.6 mm and 2 mm, respectively, showing uniform distribution of fracture process zone around the crack tip. Also, a larger fracture process zone is observed in the flattened Brazilian test. The ratio of fracture process zone volume to the total volume of sample according to the normal tensile stress criterion in Brazilian and flattened Brazilian tests is 0.35 and 0.55 percent, respectively. The extents of fracture process zone, determined based on the two criteria, are depicted in Fig. 28.

The large yield zone observed in Fig. 28c,d can be attributed to the fact that the adopted von-Mises criterion cannot distinguish between the compressive and tensile equivalent stresses, generated from the external loading and the tensile crack tip stress, respectively. As a result, the von-Mises criterion should not be adopted for these two tests.

An important note in both tests is that although the fracture toughness can be computed for a sharp and narrow crack, it is calculated at the point where stable crack growth starts. This stability is due to crack reaching to the vicinity of boundaries (loading surfaces) at the point of calculating the fracture toughness. Therefore, BDT test is not an appropriate test to determine the fracture toughness due to: lack of uniform load distribution on the sample, using the infinite plate assumption for calculation of fracture toughness, initiation of fractures from the lateral surfaces and elongated crack close to the boundaries at the point of calculation of fracture toughness. In contrast, the FBD test is more appropriate than the BDT test for determining the fracture toughness because of uniform distribution of load on the sample, using the finite plate assumption to determine the fracture toughness and the initiation of fracture from the center of sample. Nevertheless, the fracture toughness in this test is similarly affected by the boundary conditions due to the development of long crack.

5.4. General comparison of samples

Values of fracture toughness obtained from different methods differ by 42%. The maximum value is obtained from the CB test while the lowest belongs to the SCB test.

The tests can be divided into two categories: samples without a notch and samples with a notch. Without notch tests include the BDT and FBD tests. The BDT test predicts unreliable values for the fracture toughness, whereas the FBD test generates more reliable values.

According to the von-Mises criterion, the fracture process zone around the notched samples is a dumbbell-shape. In case of samples without the notch, the size of the fracture process zone is not reliably obtained by this criterion due to long crack length and the direct effect of boundaries. Moreover, the size of the fracture process zone around the crack tip in notched samples is obtained larger based on the normal tensile stress criterion than the von-Mises criterion.

In tests with a straight notch, i.e. SECRBB, SNDB, and SCB, the crack growth is unstable. Among them, the SECRBB and SCB tests provide the highest and lowest values of fracture toughness, respectively. It is recommended that the loading-unloading cycles be applied for pre-cracking of samples with straight notch [15] because pre-cracking a sample leads to a sharp and narrow crack at the tip of the notch. However, pre-cracking of rock samples is difficult due to their brittle behavior. An important factor that plays a role on evaluation of fracture toughness values in these three tests is the support span. Longer support span reduces the effects of boundary conditions in bending tests. The support span has the largest value in the SECRBB test while it remains similar in the other two tests. Despite the fact that in the SNDB and SCB

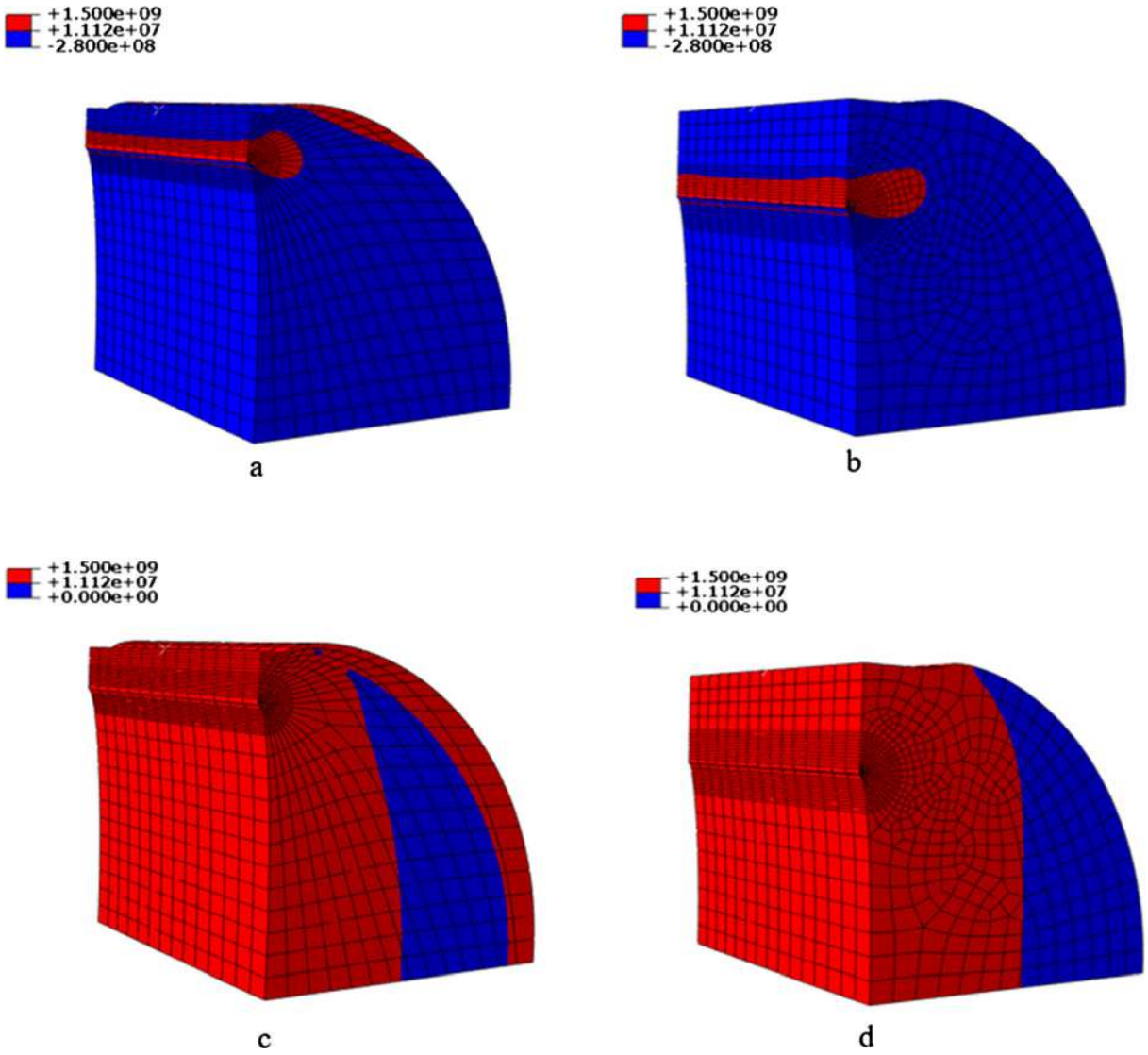

Fig. 28. Numerically predicted fracture process zones, (a) BDT samples based on the normal tensile stress criterion (b) FBD samples based on the normal tensile stress criterion, (c) BDT samples based on the von-Mises criterion and (d) FBD samples based on the von-Mises criterion (The red zone around the crack tip is the FPZ). (For interpretation of the references to colour in this figure legend, the reader is referred to the web version of this article.)

Table 4
Comparison of the fracture toughness derived from different tests with the CB test.

Test	Fracture toughness (MPa.$\sqrt{m}$)	Deviation from the CB test (%)	Source of deviation
CB	2.72	–	
SECRBB	2.29	15.81	Larger fracture process zone and unstable crack growth
FBD	2.20	19.12	Effects of boundaries on the crack growth due to long crack
SNDB	1.97	27.57	Larger fracture process zone, unstable crack growth, and the effects of boundaries due to the shorter span
SCB	1.58	41.91	Larger fracture process zone, unstable crack growth, and the effects of boundaries due to the shorter span
BDT	4.75	74.63	Non-uniform load distribution, initiating crack from boundaries rather than the center of the sample, infinite plate assumption, and effects of boundaries because of the long crack length

tests the span length is the same, different levels of fracture toughness are obtained due to the larger size of the fracture process zone in the SCB test.

Another factor that makes a difference in tests with a straight notch is the ratio of size of the fracture process zone around the crack tip to the total size of sample. This ratio in SECRBB and SNDB samples is lower than SCB samples. Furthermore, there is insignificant difference between the size of fracture process zone of SNDB and SECRBB samples due to the low volume of the fracture process zone in these tests, so these two tests are better adapted with the linear elastic assumption. Wei et al [34] showed experimentally and numerically that the large FPZ around the crack tip in the SCB test is in fact the main reason responsible for its lower fracture toughness compared with the CCNBD test. Considering two important factors that include effects of boundaries which is reduced by the longer support distance, and the size of the fracture process zone around the crack tip, the SECRBB test demonstrates more reliable values among the straight notch tests.

General comparison of tests shows that the distribution of fracture

process zone around the crack tip varies in the chevron notch samples while it approximately remains uniform in other tests. Therefore, application of the effective crack length for determination of the fracture toughness in the chevron notch samples overestimates this parameter.

In general, CB is the best test among the studied tests to determine the fracture toughness due to stable crack growth, which makes a sharp and narrow crack at the top of notch before calculating the fracture toughness, and lower size of the fracture process zone around the crack tip. Also, the boundaries have the least influence on the crack behavior in this test. Accordingly, variations of the fracture toughness of different tests are compared with the CB test in Table 4. It should be noted that the numerical results in BDT, FBD, and SNDB tests are included in this table due to either lack of an analytical solution or a more reliable 3D-finite element solution.

6. Conclusion

In this study, six tests of CB, SECRBB, SCB, SNDB, BDT and FBD have been investigated experimentally and numerically, so the following conclusions can be made:

- The results of fracture toughness show a maximum difference of 42% between various tests. The highest and lowest values are observed in CB and SCB tests, respectively.
- Among the fracture toughness tests, a suitable agreement (difference less than 8%) is observed between 3D finite element modeling of CB, SECRBB and SCB tests with equations presented earlier in order to determine the fracture toughness. Due to the infinite plate assumption in determination of fracture toughness in the BDT test and finite dimensions of Brazilian disk, there is a significant difference between the numerical results and analytical solutions. In the FBD test, the results of numerical modeling are closer to the reference results [30] (only 5.3% difference).
- To determine the fracture process zone in the samples, two criteria of uniaxial normal tensile stress and multi-axial von-Mises can be adapted. It is noted that in the case of notched samples, the fracture process zone obtained by the normal tensile stress criterion is higher than that of the von-Mises criterion. However, in the samples without a notch, the von-Mises criterion is not reliable due to long crack length and its proximity to the loading surfaces.
- The shape of the fracture process zone around the notched samples based on the von-Mises criterion becomes dumbbell-shape. However, in samples without a notch, this shape cannot be achieved due to the long crack length and its proximity to the loading surfaces.
- CB samples produce more accurate values for fracture toughness compared with SECRBB samples due to its stable crack growth which creates sharp and narrow crack at the tip of the notch and a smaller fracture process zone.
- Both SCB and SNDB tests have unstable crack growth. But, due to smaller fracture process zone in the SNDB test, more reliable values for the fracture toughness are obtained.
- Despite the fact that the growth of sharp and narrow crack occurs in the BDT test, it is not appropriate for determining the fracture toughness due to non-uniform distribution of load on the sample, initiation of crack from the loading surfaces, assumption of infinite plate to derive an equation for the fracture toughness, long cracking and the effect of boundaries at the point of calculating the fracture toughness. Although most of the flaws of the BDT test have been eliminated in the FBD test, the results remain directly affected by boundaries.
- In the case of straight notch tests which show an unstable crack growth, the SECRBB test provides more accurate values for the fracture toughness than the SCB and SNDB tests. This is because of the small ratio of the volume of fracture process zone at the crack tip to the total sample volume. Moreover, the SECRBB test is less influenced by the boundaries according to its longer support span.
- General comparison of the fracture process zone distribution around the crack tip shows that this distribution is non-uniform around the chevron notch samples, although it approximately remains uniform along the crack tip in other tests. Therefore, application of the effective crack length for calculating the fracture toughness of chevron samples leads to over estimation.
- CB is the best test to determine fracture toughness of rocks amongst all the mentioned methods due to its stable crack growth, which results in creating a sharp and narrow crack at the top of notch, and the small size of the fracture process zone around the crack tip. Furthermore, the boundary conditions do not have any considerable effect on crack behavior.

Acknowledgement

The authors wish to acknowledge the Rock Mechanics Laboratory at the School of Mining Engineering, University of Tehran, for assistance in conducting the experiments; with special thanks to Mr. Mohammad Hoveidafar.

References

[1] V.E. Saouma, Fracture Mechanics, Univesity of Colorado, USA, 2000.
[2] F. Ouchterlony, ISRM commission on testing method; suggested methods for determining fracture toughness using chevron bend specimens, Int. J. Rock Mech. Min. Sci. Geomech. Abstr. 25 (1988) 71–96, https://doi.org/10.1016/0148-9062(88)91871-2.
[3] S. Mohammadi, Extended Finite Element Method for Fracture Analaysis of Structures, first ed., Blackwell Publishing, UK, 2008.
[4] L. Tutluoglu, C. Keles, Mode I fracture toughness determination with straight notched disk bending method, Int. J. Rock Mech. Min. Sci. Geomech. Abstr. 48 (2011) 1248–1261, https://doi.org/10.1016/j.ijrmms.2011.09.019.
[5] A.J. Bush, Experimentally determined stress intensity factors for single-edge-crack round bars loading in bending, Exp. Mech. 16 (1976) 249–257, https://doi.org/10.1007/BF02321148.
[6] F. Ouchterlony, Extension of the compliance and stress intensity formulas for the single edge crack round bar in bending, in: S.W. Freiman, E.R. Fuller (Eds.), Fracture mechanics methods for ceramics, rocks, and concrete, 1981, pp. 237–256, , https://doi.org/10.1520/STP28309S.
[7] M.-D. Wei, F. Dai, N.-W. Xu, Y. Liu, T. Zhao, A novel chevron notched short rod bend method for measuring the mode I fracture toughness of rocks, Eng. Fract. Mech. (2017), https://doi.org/10.1016/j.engfracmech.2017.11.041.
[8] M.D. Kuruppu, Y. Obara, M.R. Ayatollahi, K.P. Chong, T. Funatsu, commission on testing method; suggested method for determining the mode I static fracture toughness using semi-circular bend specimen, Rock. Mech. Rock. Eng. 47 (2014) 267–274, https://doi.org/10.1007/s00603-013-0422-7.
[9] M.D. Kuruppu, Fracture toughness measurement using chevron notched semi-circular bend specimen, Int. J. Fract. 86 (1997) 33–38.
[10] H. Guo, N.I. Aziz, L.C. Schmidt, Rock fracture-toughness determination by the Brazilian test, Eng. Geol. 33 (1993) 177–188, https://doi.org/10.1016/0013-7952(93)90056-I.
[11] Q.Z. Wang, L. Xing, Determination of fracture toughness K_{IC} by using the flattened Brazilian disk specimen for rocks, Eng. Fract. Mech. 64 (1999) 193–201, https://doi.org/10.1016/S0013-7944(99)00065-X.
[12] H. Awaji, S. Sato, Combined mode fracture toughness measurements by the disc test, J. Eng. Master Tech. Trans. ASME 100 (1978) 175–182, https://doi.org/10.1115/1.3443468.
[13] M. Thiercelin, J.C. Roegiers, Fracture toughness determination with the modified ring test, Proceedings of the international symposium on engineering in complex rock formations, Beijing, 1986, pp. 1–8.
[14] R.J. Fowell, ISRM commission on testing method: suggested method for determining mode I fracture toughness using cracked chevron notched brazilian disc (CCNBD) specimens, Int. J. Rock Mech. Min. Sci. Geomech. Abstr. 32 1955, pp. 57–64, , https://doi.org/10.1016/0148-9062(94)00015-U.
[15] Z. Sun, F. Ouchterlony, Fracture toughness of stripa granite cores, Int. J. Rock. Mech. Min. Sci. Geomech. Abstr. 23 (1986) 399–409, https://doi.org/10.1016/0148-9062(86)92305-3.
[16] K. Khan, N.A. Al-Shayea, Effect of specimen geometry and testing method on mixed mode I-II fracture toughness of a limestone rock from Saudi Arabia Rock, Mech. Rock. Eng. 33 (2000) 179–206, https://doi.org/10.1007/s006030070006.
[17] S.H. Chang, I.L. Chung, S. Jeon, Measurement of rock fracture toughness under modes I and II and mixed-mode conditions by using disc-type specimens, Eng. Geol. 66 (2002) 79–97, https://doi.org/10.1016/S0013-7952(02)00033-9.
[18] M.J. Iqbal, B. Mohanty, Experimental calibration of stress intensity factors of the ISRM suggested cracked chevron-notched Brazilian disc specimen used for determination of mode-I fracture toughness, Int. J. Rock Mech. Min. Sci. 43 (2006) 1270–1276, https://doi.org/10.1016/j.ijrmms.2006.04.014.
[19] M.J. Iqbal, B. Mohanty, Experimental calibration of ISRM suggested fracture

toughness measurement techniques in selected brittle rocks, Rock Mech. Rock Eng. 40 (453–475) (2007) 1270–1276, https://doi.org/10.1007/s00603-006-0107-6.
[20] Q.Z. Wang, Formula for calculating the critical stress intensity factor in rock fracture toughness tests using cracked chevron notched Brazilian disc (CCNBD) specimens, Int. J. Rock Mech. Min. Sci. 47 (2010) 1006–1011, https://doi.org/10.1016/j.ijrmms.2010.05.005.
[21] Q.Z. Wang, X.P. Gou, H. Fan, The minimum dimensionless stress intensity factor and its upper bound for CCNBD fracture toughness specimen analyzed with straight through crack assumption, Eng. Fract. Mech. 82 (2012) 1–8, https://doi.org/10.1016/j.engfracmech.2011.11.001.
[22] Z. Cui, D. Liu, G. An, B. Sun, M. Zhou, F. Cao, A comparison of two ISRM suggested chevron notched specimens for testing mode-I rock fracture toughness, Int. J. Rock Mech. Min. Sci. 47 (2010) 871–876, https://doi.org/10.1016/j.ijrmms.2009.12.015.
[23] F. Dai, M.D. Wei, N.W. Xu, Y. Ma, D.S. Yang, Numerical assessment of the progressive rock fracture mechanism of cracked chevron notched Brazilian disc specimens, Rock Mech. Rock Eng. 48 (2015) 463–479, https://doi.org/10.1007/s00603-014-0587-8.
[24] M.-D. Wei, F. Dai, N.-W. Xu, T. Zhao, Experimental and numerical investigation of cracked chevron notched Brazilian disc specimen for fracture toughness testing of rock, Fatigue Fract. Eng. Mater. Struct. 41 (2018) 197–211, https://doi.org/10.1111/ffe.12672.
[25] M.-D. Wei, F. Dai, N.-W. Xu, T. Zhao, Stress intensity factors and fracture process zones of ISRM-suggested chevron notched specimens for mode I fracture toughness testing of rocks, Eng. Fract. Mech. 168 (2016) 174–189, https://doi.org/10.1016/j.engfracmech.2016.10.004.
[26] T. Funatsu, N. Shimizu, M. Kuruppu, K. Matsui, Evaluation of mode I fracture toughness assisted by the numerical determination of K-resistance, Rock Mech. Rock Eng. 48 (2015) 143–157, https://doi.org/10.1007/s00603-014-0550-8.
[27] M.D. Wei, F. Dai, N.W. Xu, Y. Xu, K. Xia, Three-dimensional numerical evaluation of the progressive fracture mechanism of cracked chevron notched semi-circular bend rock specimens, Eng. Fract. Mech. 134 (2015) 286–303, https://doi.org/10.1016/j.engfracmech.2014.11.012.
[28] M.D. Wei, F. Dai, N.W. Xu, J.F. Liu, J. Xu, Experimental and numerical study on the cracked chevron notched semi-circular bend method for characterizing the mode I fracture toughness of rocks, Rock Mech. Rock Eng. 49 (2016) 1595–1609, https://doi.org/10.1007/s00603-015-0855-2.
[29] Q.Z. Wang, X.M. Jia, S.Q. Kou, Z.X. Zhang, P.A. Lindqvist, The flattened Brazilian disc specimen used for testing elastic modulus, tensile strength and fracture toughness of brittle rocks: analytical and numerical results, Int. J. Rock Mech. Min. Sci. 41 (2004) 245–253, https://doi.org/10.1016/S1365-1609(03)00093-5.
[30] C. Keles, L. Tutluoglu, Investigation of proper specimen geometry for mode I fracture toughness testing with flattened Brazilian disc method, Int. J. Fract. 69 (2011) 61–75, https://doi.org/10.1007/s10704-011-9584-z.
[31] J. Justo, J. Castro, S. Cicero, M.A. Sánchez-Carro, R. Husillos, Notch effect on the fracture of several rocks: application of the theory of critical distances, Theoretical Appl. Fract. Mech. (2017), https://doi.org/10.1016/j.tafmec.2017.05.025.
[32] D. Taylor, The theory of critical distances: a link to micromechanisms, Theoretical Appl. Fract. Mech. 90 (2017) (2017) 8–13, https://doi.org/10.1016/j.tafmec.2017.05.018.
[33] M.D. Wei, F. Dai, N.W. Xu, T. Zhao, Y. Liu, An experimental and theoretical assessment of semi-circular bend specimens with chevron and straight-through notches for mode I fracture toughness testing of rocks, Int. J. of Rock Mech. Min. Sci. 99 (2017) 28–38, https://doi.org/10.1016/j.ijrmms.2017.09.004.
[34] M.D. Wei, F. Dai, N.W. Xu, T. Zhao, K.W. Xia, Experimental and numerical study on the fracture process zone and fracture toughness determination for ISRM-suggested semi-circular bend rock specimen, Eng. Fract. Mech. (2016), https://doi.org/10.1016/j.engfracmech.2016.01.002.